Available online at www.sciencedirect.com
SCIENCE DIRECT®
Journal of Nuclear Materials 335 (2004) 387–396
journal of nuclear materials
www.elsevier.com/locate/jnucmat

Delayed hydride cracking in Zr–2.5Nb tube with the cooling rate and the notch tip shape

Young Suk Kim *, Sang Jai Kim, Kyung Soo Im

Zirconium Team, Korea Atomic Energy Research Institute, P.O. Box 105, Yusong, Daejeon 305-353, Korea

Received 14 April 2003; accepted 20 July 2004

Abstract

The objective of this study is to demonstrate the feasibility of the Kim's delayed hydride cracking (DHC) model. To this end, this study has investigated the velocity and incubation time of delayed hydride cracking (DHC) for the water-quenched and furnace-cooled Zr–2.5Nb tubes with a different radius of notch tip. DHC tests were carried out at constant K_I of 20 MPa $\sqrt{m}$ on cantilever beam (CB) specimens subjected to furnace cooling or water quenching after electrolytic charging with hydrogen. An acoustic emission sensor was used to detect the incubation time taken before the start of DHC. The shape of the notch tip changed from fatigue cracks to smooth cracks with its tip radius ranging from 0.1 to 0.15 mm. The DHC incubation time increased remarkably with the increased radius of the notch tip, which appeared more strikingly on the furnace-cooled CB specimens than on the water-quenched ones. However, both furnace-cooled and water-quenched CB specimens indicated little change in DHC velocity with the radius of the notch tip unless their notch tip exceeded 0.125 mm. These results demonstrate that the nucleation rate of hydrides at the notch tip determines the incubation time and the DHC velocity becomes constant after the concentration of hydrogen at the notch tip reaches terminal solid solubility for dissolution (TSSD), which agrees well with the Kim's DHC model. A difference in the incubation time and the DHC velocity between the furnace-cooled and water-quenched specimens is attributed to the nucleation rate of reoriented hydrides at the notch tip and the resulting concentration gradient of hydrogen between the notch tip and the bulk region.

PACS: 81.40.Np

1. Introduction

Though delayed hydride cracking (DHC) has been recognized as one of the Zr–2.5Nb tube failures since the 1970s, its full understanding has yet to be made. Dutton and Puls suggested for the first time that a main driving force for DHC is the stress gradient between the notch and the bulk region far away from it, which has been acknowledged as a rational hypothesis for now [1,2]. However, their DHC model has some defects: firstly, it cannot explain why DHC velocity becomes constant regardless of the applied stress intensity factor even though the stress gradient is affected by the applied stress intensity factor at the notch tip [3], secondly, it cannot explain why DHC velocity has a strong dependency on the way how we approach the test tem-

* Corresponding author. Tel.: +82 42 868 2359; fax: +82 42 868 8346.
E-mail address: yskim1@kaeri.re.kr (Y.S. Kim).

0022-3115/$ - see front matter © 2004 Elsevier B.V. All rights reserved.
doi:10.1016/j.jnucmat.2004.07.046

perature by cooling-down or heating-up even under the same stress gradient [4] and thirdly, it can not predict any hydride size effect on the DHC velocity [5]. Recently, Kim et al. suggested another DHC model details of which is schematically illustrated as shown in Fig. 1 [6,7]. During heating-up to the peak temperature, the Zr–2.5Nb specimen has hydrogen dissolved in the zirconium matrix whose maximum concentration follows the terminal solid solubility for dissolution (TSSD) while during cool-down the dissolved hydrogen concentration of the specimen follows the terminal solid solubility for precipitation (TSSP) [8]. Thus, when the Zr–2.5Nb specimen containing 60 ppm H, for example, is heated up to 310 °C (A point) and cooled down to the temperature, 250 °C (B point) without applied tensile stress as shown in Fig. 1, the specimen still has most of hydrogen (corresponding to the B point as shown in Fig. 1) dissolved in the zirconium matrix, leading the zirconium matrix to become supersaturated with hydrogen. When the tensile stress is applied to the Zr–2.5Nb specimen with a notch, the work energy given by the tensile stress can compensate for the lattice strain energy caused by the precipitation of the hydrides with a larger volume in the zirconium matrix with a smaller volume [9]. In other words, the applied tensile stress acts to trigger the nucleation of the hydrides only at the notch tip, reducing the supersaturated hydrogen concentration. Since the notch tip is exposed continuously to the tensile stress at the constant test temperature for a long time, the continuous precipitation of the hydrides at the notch tip will reduce the supersaturated hydrogen concentration there to the equilibrium hydrogen concentration corresponding to the C point. Since the bulk region far away from the notch tip still maintains the supersaturated hydrogen concentration due to little effect of the applied tensile stress, there develops a gradient of the hydrogen concentration between the notch tip and the bulk region (corresponding to the distance BC as shown in Fig. 1), which is a driving force for inducing DHC.

Thus, it is the radius of the crack tip and the supersaturated hydrogen concentration in the zirconium matrix that are the critical factors in determining the nucleation rate of hydrides at the crack tip under the applied tensile stress. The smaller the radius of the crack and the larger the supersaturated hydrogen concentration in solution, the shorter the incubation time and the larger the velocity of the DHC will become. One way to change the amount of the supersaturated hydrogen concentration in solution even at the same concentration of charged hydrogen is to change the size of hydrides precipitated in the Zr–2.5Nb specimens by changing the cooling rate during their cooling following homogenization heat treatment. It is because the Zr–2.5Nb with coarser hydrides will have the lesser concentration of dissolved hydrogen during a thermal cycle [10,11] where the test temperature is approached by cooling from the peak temperature. Thus it is expected that the Zr–2.5Nb with coarser hydride precipitates will need a longer incubation time and lower DHC velocity.

Therefore, the objective of this study is to verify the feasibility of the Kim's DHC model by looking into the effect of the hydride size and the radius of the notch tip on the incubation time and velocity of DHC. To these ends, the crack tip radius changed from sharp cracks like a fatigue crack to smooth cracks with the tip radius of 0.1, 0.125 and 0.15 mm, respectively while the size of precipitated hydrides changed by subjecting the Zr–2.5Nb cantilever beam specimens to water quenching or furnace cooling after homogenization treatment.

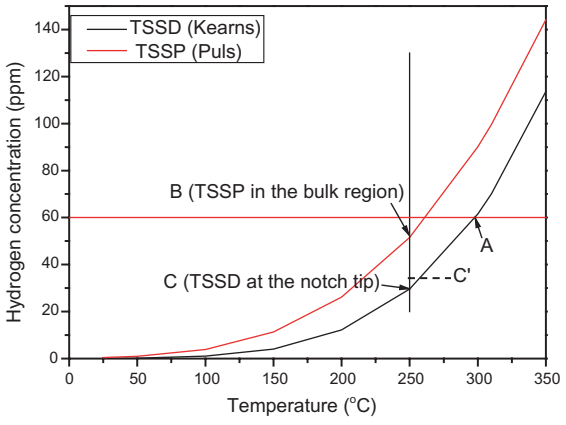

Fig. 1. Terminal solid solubility of hydrogen during heating-up and cooling-down of Zr–2.5Nb specimens with a notch.

2. Experimental procedures

2.1. Material

The cantilever beam (CB) specimens of 3.2 mm wide and 38 mm long were cut out of a CANDU Zr–2.5Nb tube (used in the Wolsong NPS) subjected to heat treat-

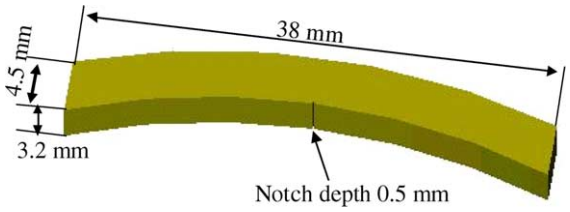

Fig. 2. Schematic diagram of the cantilever beam (CB) specimens taken from a CANDU Zr–2.5Nb tube.

ment at 400 °C for 24 h after cold working as shown in Fig. 2. They had smooth and sharp notches of 0.5 mm depth in the radial direction of the tube: the smooth notches had a radius of tip ranging from 0.1, 0.125 and 0.15 mm, respectively as shown in Fig. 3 while a sharp notch corresponded to a pre-fatigue crack that was grown by 0.5 mm from the notch using a 3-point bending method. The CB specimens were subjected to electrolytic charging to form a thick hydride layer on their surfaces followed by homogenization treatment at 302 °C for 30 h to theoretically contain 60 ppm H [12,13] and then were water-quenched or furnace-cooled to change the size of hydride precipitates from fine to coarse as shown in Fig. 4. Details of the hydrogen charging methods are reported elsewhere [12]. Using a LECO RH 404 analyzer, the actual hydrogen concentrations of the water-quenched (WC) and furnace-cooled (FC) specimens were determined to have 72 and 57 ppm H, respectively, corresponding to an average of 5–7 measured data set.

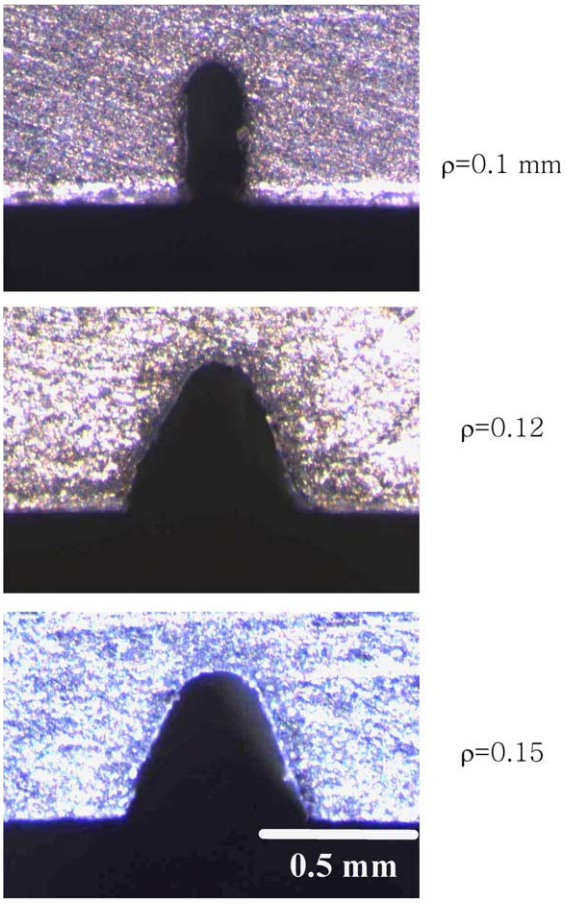

Fig. 3. Cantilever beam specimens with the notch tip radius, ρ ranging from 0.1 to 0.15 mm.

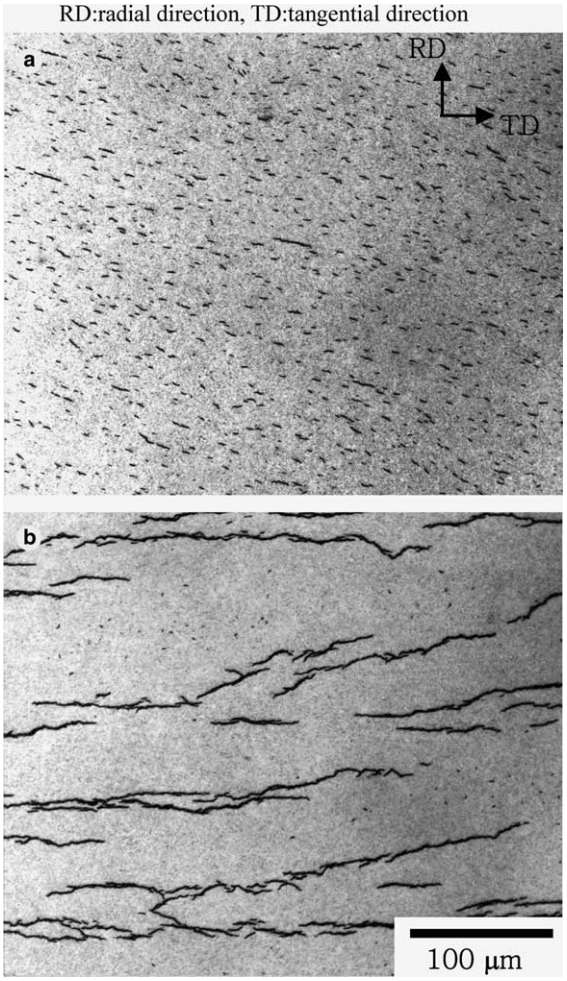

Fig. 4. (a) Fine hydrides in the water-quenched and (b) coarser hydrides in the furnace-cooled Zr–2.5Nb CB specimens.

2.2. DHC tests

DHC tests were conducted only at 250 °C using cantilever beam testers attached with an acoustic emission (AE) sensor as shown in Fig. 5. The temperatures of the specimens were directly monitored and controlled with a K-type thermocouple welded to the CB specimens. During DHC tests, a thermal cycle was applied to approach the test temperature by cooling from the peak temperature; all the FC and WQ specimens were heated up at a rate of 0.5–5 °C/min to the peak temperature of 310 °C for 1 h to get the hydrides dissolved in zirconium followed by cooling-down to the test temperature of 250 °C at a rate of 1–2 °C/min. At least 30 min after the specimens reach 250 °C, the constant stress intensity factor of 20 MPa $\sqrt{m}$ was applied to all the CB specimens and was kept constant through an auto-control program where applied load is reduced in

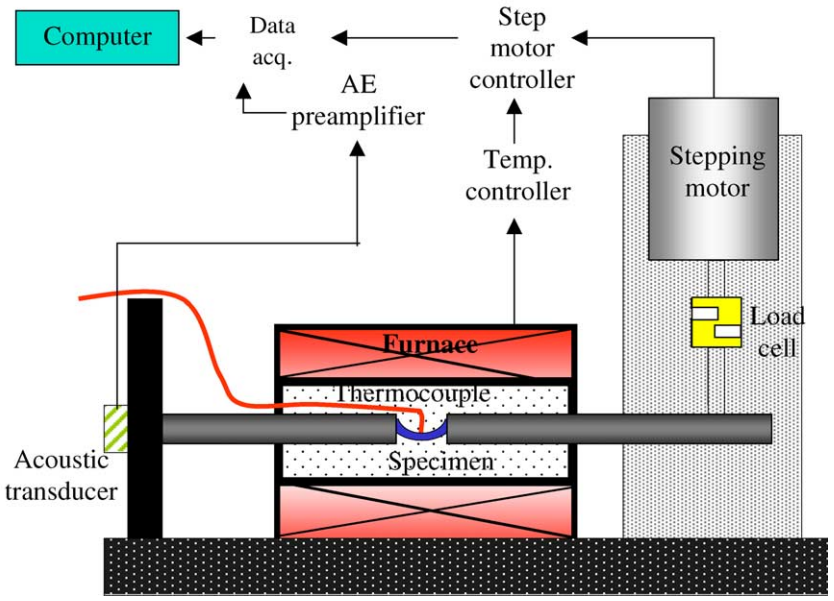

Fig. 5. Schematic diagram of the testing equipment used for DHC tests with an acoustic emission sensor to determine the initiation and growth of the DHC crack.

proportion to the crack length obtained from the cumulative AE counts using a step-motor. A more detailed method to maintain the applied stress intensity factor constant is described elsewhere [14,15]. Here, the applied stress intensity factor, K_I was defined as such [4,12]:

$$K_I = \frac{4.12M\sqrt{X^{-3} - X^3}}{B(D^{3/2})},$$

where M is the bending moment (= the sum of the grip weight times the center gravity of the lever bar plus applied load times the distance from the notch to the loading point), B is the width of the specimen, D is its thickness, A is the notch depth and $X = 1 - A/D$. It is to note that the stress intensity factor is determined by the dimension of the CB specimen, the notch depth (= 0.5 mm) and the applied load including the grip weight independent of the notch tip radius. Thus, by applying the same stress intensity factor to the CB specimens with a different notch tip radius, we changed the tensile stress applied to the notch tip as a function of the notch tip radius.

The incubation time was defined as a period of time from the zero time when the load was applied for the first time to the time when the first AE signal was picked up from the CB specimens while the crack velocity was obtained from the average crack length divided by the time over which the stable crack grew.

3. Results and discussion

3.1. DHC incubation time with the notch tip radius and the cooling rate

Figs. 6 and 7 show the AE counts and load with time during DHC tests on the furnace-cooled and water-quenched specimens at 250 °C. Regardless of the different shape of the notch tip, all the specimens successfully had the DHC crack growth as shown in Fig. 8 where typical DHC fracture patterns are shown for the furnace-cooled and water-quenched specimens. Based on the acoustic emission signals picked up as shown in Figs. 6 and 7, the incubation time of DHC was plotted as a function of the notch tip radius as shown in Fig. 9. Both the specimens had a gradual increase in the incubation time with the increased radius of the notch tip up to a tip radius of 0.125 mm. However, at the notch tip radius of 0.15 mm, there is a sharp increase in the incubation time, leading to a notable difference in the incubation time between the furnace-cooled and water-quenched specimens: the furnace-cooled specimen has a longer incubation time than the water-quenched one.

According to the Kim's DHC model, it is the nucleation rate of hydrides at the notch tip that determines the incubation time of DHC. It is because a concentration gradient driving DHC is developed only after the nucleation of the hydrides. Generally, the nucleation rate of the hydrides will depend on the texture determining a distribution of the hydride habit planes, the super-

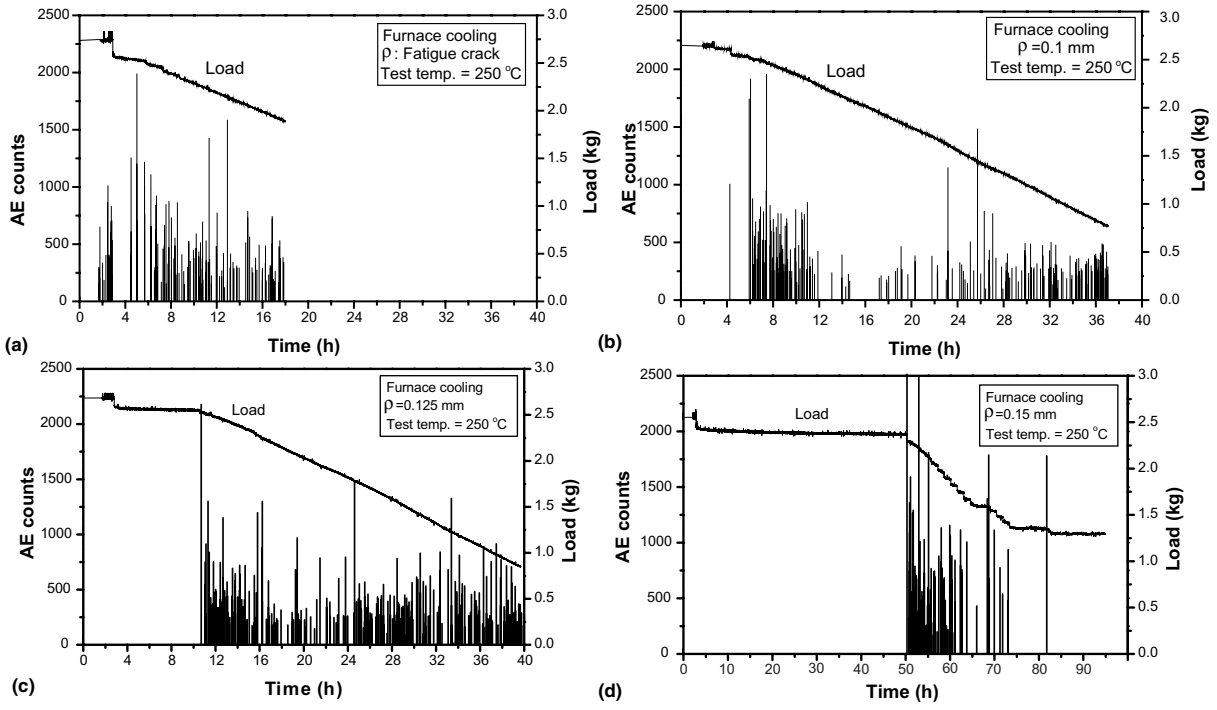

Fig. 6. Acoustic emission counts and load with time for the furnace-cooled CB specimens with different notch tip radii during DHC tests at 250 °C: (a) fatigue crack and (b), (c), (d) the notch tip radius of 0.1, 0.12 and 0.15 mm, respectively.

saturated hydrogen concentration and an applied tensile stress to the notch tip. Since we have used the Zr–2.5Nb specimens with a constant texture and the similar hydrogen concentration, it is the applied tensile stress to greatly influence the nucleation rate of the hydrides. Since the same stress intensity factor has been applied to all the specimens during DHC tests, the applied tensile stress at the notch tip becomes smaller with the larger notch tip radius, slowing down the nucleation rate of the hydrides at the notch tip (called the enhanced nucleation of the hydrides by the stress effect). Hence, the longer DHC incubation time for both the specimens with the larger tip radius of the notch demonstrates that the nucleation rate of hydrides at the crack tip region governs the incubation time.

Another thing to note is that the furnace-cooled specimen with coarser hydrides needs longer incubation time especially at a notch tip radius exceeding 0.1 mm than the water-quenched one with fine hydrides. There are two factors that the size of hydrides can affect: firstly, the terminal solid solubility for dissolution and precipitation, and secondly, the nucleation of reoriented hydrides under tensile stress at the test temperature. Since fine hydrides in the water-quenched specimen (as shown in Fig. 4) are likely to be under high elastic constraint compared to coarse hydrides in the furnace cooled one (as shown in Fig. 4) that are accommodated more plastically [5,9–11,16,17], the terminal solid solubility for dissolution will shift toward an increase in the dissolved hydrogen concentration for the water-quenched specimen with fine hydrides as shown in Fig. 10 compared to that of the furnace-cooled one. This rationale is based on the Puls's suggestion that the TSSD is determined by plastic accommodation energy resulting from the hydride-matrix misfit and the TSSP is determined by elastic accommodation effects [16]. Further, during cooling-down to the test temperature at the same rate, a memory effect will cause fine hydrides and coarse hydrides to precipitate in the water-quenched specimen and in the furnace-cooled specimen, respectively [10]. It is because the water-quenched specimen will have left a few dislocations at the sites occupied by fine hydrides because of high elastic misfit stresses, facilitating the homogeneous nucleation of the hydrides during the cooling-down [10] and requiring a larger undercooling before the nucleation of hydrides [8,9]. The homogeneous nucleation of the hydrides will contribute to the higher misfit strain energy, leading the water-quenched specimens to have a higher TSSP [16]. By contrast, the furnace-cooled specimen will have lots of dislocations generated at the sites occupied by very large hydrides, facilitating a heterogeneous nucleation of the hydrides at the dislocations created at the sites occupied by very coarse hydrides [8,9,15–17]. Likewise,

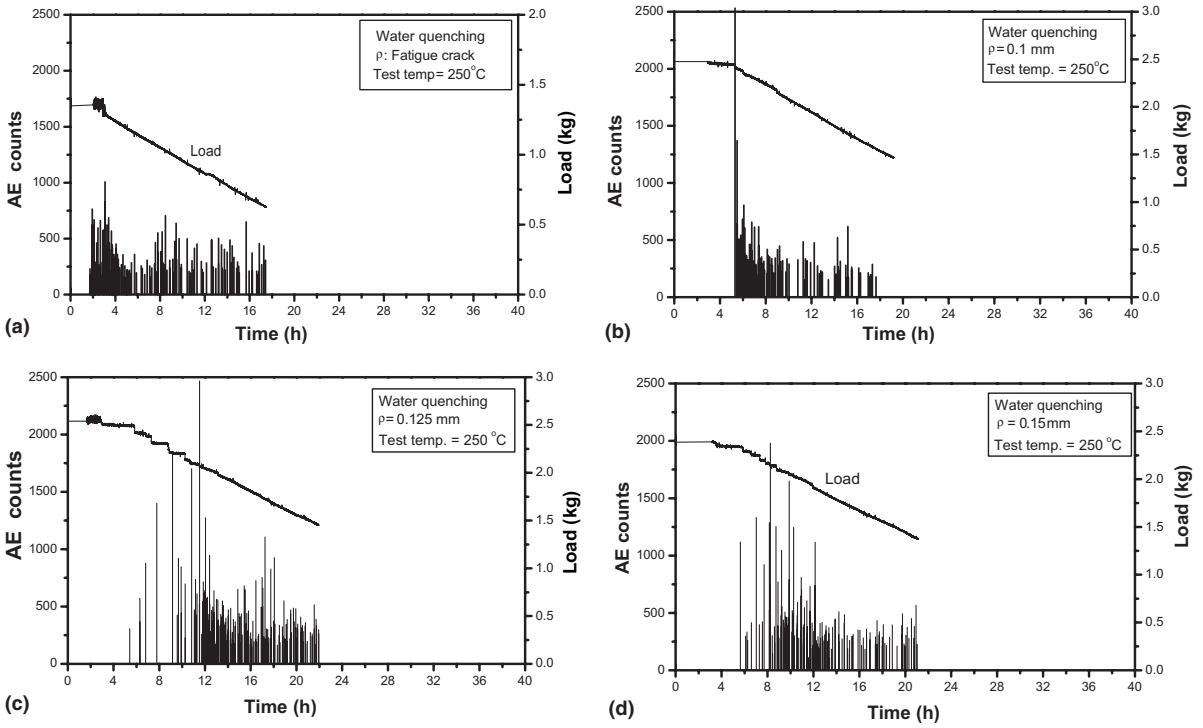

Fig. 7. Acoustic emission counts and load with time for the water-quenched CB specimens with different notch tip radii during DHC tests at 250 °C: (a) fatigue crack and (b), (c), (d) the notch tip radius of 0.1, 0.12 and 0.15 mm, respectively.

the heterogeneous nucleation of the hydrides will contribute to the lower misfit stain energy, leading the furnace-cooled specimen to have a lower TSSP compared to that of the water-quenched specimen [16]. Therefore, when the specimen is cool-down from the peak temperature to the test temperature, the water-quenched specimen will have a comparatively higher supersaturation of the dissolved hydrogen (corresponding to the B′ point as shown in Fig. 10) than that of the furnace-cooled specimen (corresponding to the B point). Under applying tensile stresses, the higher the supersaturation of the dissolved hydrogen becomes, the faster the nucleation of the reoriented hydrides, leading the water-quenched specimen to have enhanced nucleation of the reoriented hydrides and a shorter incubation time for DHC as shown in Fig. 9. By contrast, this memory effect [10] related to the precipitation of hydrides suppresses the nucleation of reoriented hydrides in the furnace-cooled specimen, likely leading it to have a longer incubation time for DHC with a strong dependency upon the notch tip radius as shown in Fig. 9 as opposed to the water-quenched one.

To provide concrete evidence for the above hypothesis, we investigated the reorientation of hydrides in the water-quenched and furnace-cooled specimens after they were cooled under a tensile stress of 200 MPa from 380 °C to 250 °C. As shown in Fig. 11, the water-quenched had many hydrides reoriented normally to the tensile stress direction across the whole section while the furnace-cooled had little reoriented hydrides even at the notch tip. Therefore, we conclude that the shorter incubation time for the water-quenched specimen is due to the enhanced precipitation of the reoriented hydrides caused by an increased supersaturation of hydrogen during cooling, demonstrating that the nucleation rate of the hydrides at the notch tip governs the incubation time for DHC. Further, this enhanced nucleation of the reoriented hydrides at the notch tip leads the water-quenched specimen to have a lesser dependency of the incubation time for DHC upon the notch tip radius as shown in Fig. 9. Conversely, it is due to a slow nucleation rate of the hydrides for the furnace-cooled specimen that their incubation time has a strong dependency upon the notch tip radius as shown in Fig. 9. Considering that a difference in the incubation time for DHC is very noticeable only at the large crack tip radius, or 0.15 mm between the water-quenched and furnace-cooled specimens, however, the enhanced nucleation of the reoriented hydrides caused by the stress effect seems to be a main governing factor for the incubation time compared to an increase in the supersaturation of hydrogen caused by the hydride size effect.

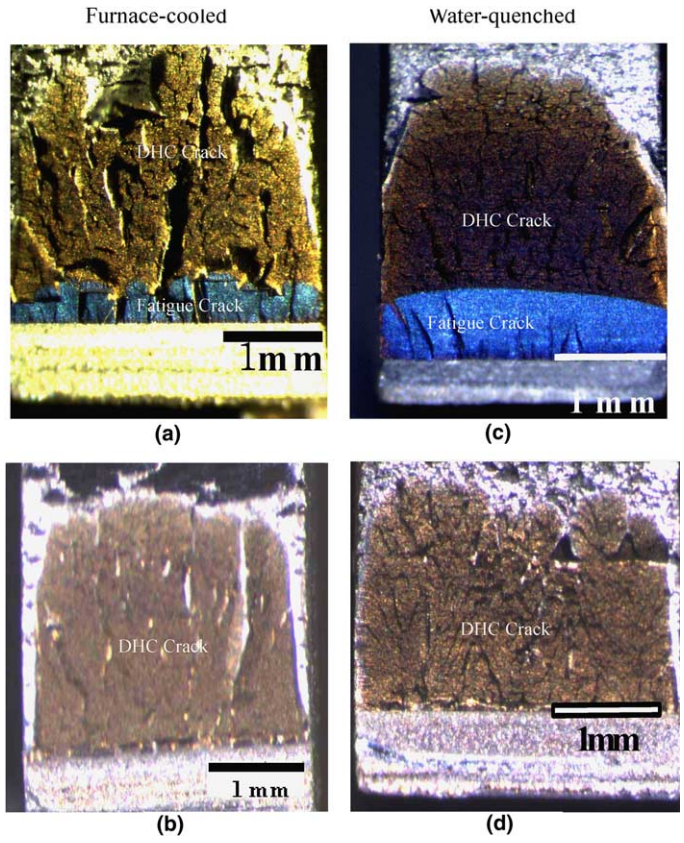

Fig. 8. Fracture pattern of the DHC cracks for the furnace-cooled (a,b) and water-quenched (c,d) cantilever beam specimens with different types of notches: (a,c) the sharp notch with a fatigue crack and (b,d) the smooth notch with the 0.125 mm tip radius.

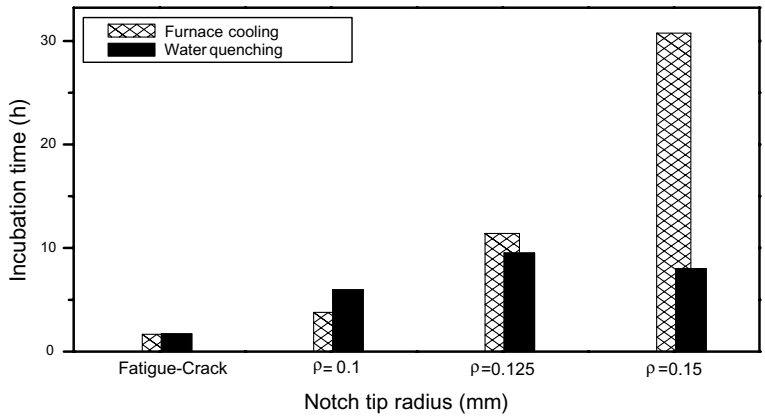

Fig. 9. Incubation time of DHC for furnace-cooled and water-quenched Zr–2.5Nb cantilever beam specimens at 250 °C.

3.2. DHC velocity with the cooling rate

Once the incubation time is reached, both CB specimens had a stable growth of DHC crack irrespective of the crack tip radius as shown in Fig. 12. The DHC velocity became constant independent of the crack tip radius when the crack tip radius is sharp enough to be less than or equal to 0.125 mm but was reduced a bit for the crack whose tip radius is larger than 0.125 mm as shown in Fig. 12. The same dependency of DHC

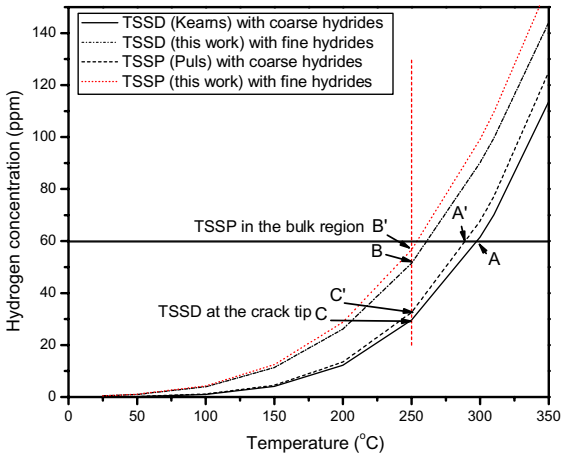

Fig. 10. Terminal solid solubility of hydrogen during heating-up and cooling-down of Zr–2.5Nb specimens with the different size of hydries.

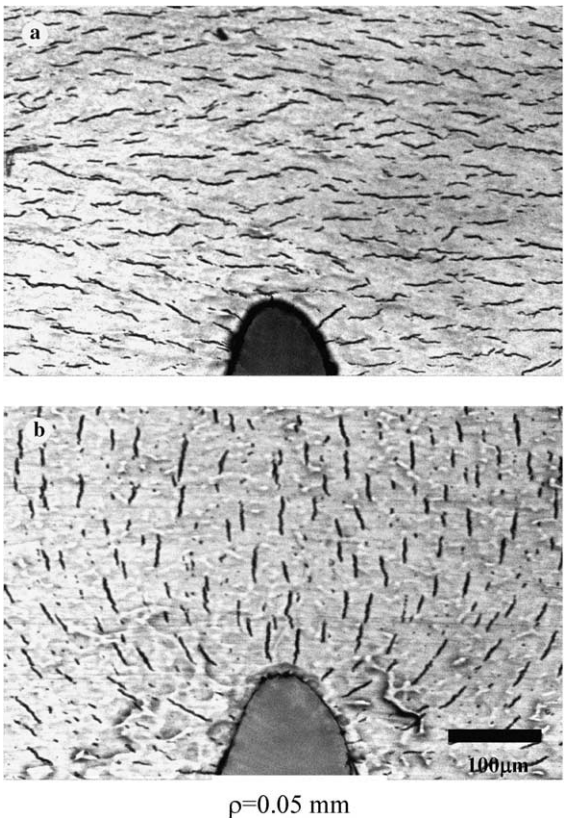

Fig. 11. Distribution of reoriented hydrides in (a) the furnace-cooled and (b) the water-quenched specimens with the 0.05 mm notch tip radius subjected to cooling under 200 MPa from 380 to 250 °C.

velocity on the crack tip radius was observed also for the water-quenched specimen. In other words, the DHC

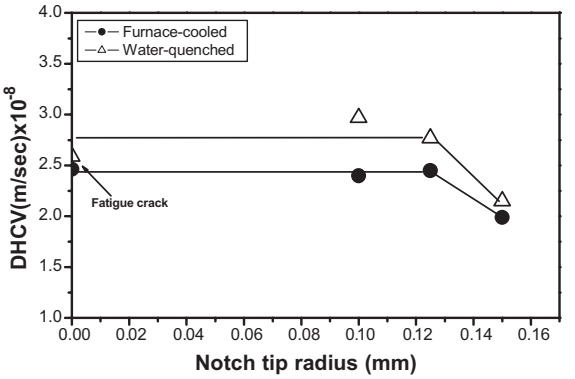

Fig. 12. Radial DHC velocity of the furnace-cooled and water-quenched cantilever beam specimens with at 250 °C with the notch tip shape.

velocity is not affected by the shape of any surface flaws unless the surface flaws are smooth enough for the tip radius to exceed 0.125 mm once the initiation of DHC has begun.

Kim's DHC model as shown in Fig. 1 suggests that the nucleation of hydrides at the crack tip reduces the supersaturated hydrogen concentration around the notch tip to the equilibrium hydrogen concentration (labeled as C in Fig. 1) or the terminal solid solubility of hydrides for dissolution. Thus, as long as the notch tip reaches the equilibrium hydrogen concentration in solution (corresponding to the C point) irrespective of the tip radius, then the constant concentration gradient is developed (the distance BC as shown in Fig. 1), leading to a constant DHC velocity irrespective of the initial notch radius and applied tensile stresses [6,7]. This explains why the water-quenched and furnace-cooled specimens have a constant DHC velocity irrespective of the notch tip radius. However, when the notch tip radius is too large for the notch tip region to reach the equilibrium hydrogen concentration in solution just as in the case of the Zr–2.5Nb CB specimens with the 0.15 mm tip radius, the hydrogen concentration the notch tip can have is higher (corresponding to the C′ point in Fig. 1) than the equilibrium hydrogen concentration (corresponding to the C point). Consequently, a gradient of the hydrogen concentration between the notch tip and the bulk region becomes the distance BC′ as shown in Fig. 1, which is smaller than the distance BC corresponding to a hydrogen concentration gradient between the notch tip and the bulk region at the equilibrium. This leads to a lower DHC velocity as shown in Fig. 12. However, as the sharp DHC crack grows ahead of the initial notch with time, then the hydrogen concentration at the tip of the crack will reach the equilibrium hydrogen concentration more easily and faster. This leads to a small difference in DHC velocity with the notch tip radius as shown in Fig. 12.

Another thing to note is that the water-quenched specimen has a slightly higher DHC velocity than the furnace-cooled one as shown in Fig. 12. This trend indicating a dependency of DHC velocity on the cooling rate agrees well with Amouzouvi's results [5] but the difference in DHC velocity between the water-quenched and furnace-cooled specimens is around 10–20% which is much smaller than that reported by Amouzouvi [5]. To confirm the dependency of DHC velocity on the cooling rate, DHC tests were again conducted on the compact tension specimens taken from the CANDU Zr–2.5Nb tube with 60 ppm H that were water-quenched or furnace-cooled after the homogenization treatment temperature at 302 °C. The same DHC test method as applied to the CB specimens was used where the stress intensity factor was applied 30 min after the test temperatures were reached by cooling from the peak temperature of 310 °C. Here, the applied stress intensity factor was 15 MPa $\sqrt{m}$ at the start of the DHC tests and then increasing continuously to around 25–27 MPa $\sqrt{m}$ with the growth of the crack. A set of 3 DHC velocity data was determined at each temperature from the water-quenched and furnace-cooled specimens, respectively. As shown in Fig. 13, the water-quenched was confirmed to have a slightly higher DHC velocity both at temperatures of 182 and 200 °C even though the difference in DHC velocity is small.

If the terminal solid solubility of hydrides for dissolution and precipitation are constant independent of the size of the hydrides, a concentration gradient between the crack tip and the bulk region is the same for the water-quenched and furnace-cooled specimens, leading to the same DHC velocity. It is because the driving force for DHC is the concentration gradient between the crack tip and the bulk region as illustrated in Fig. 1.

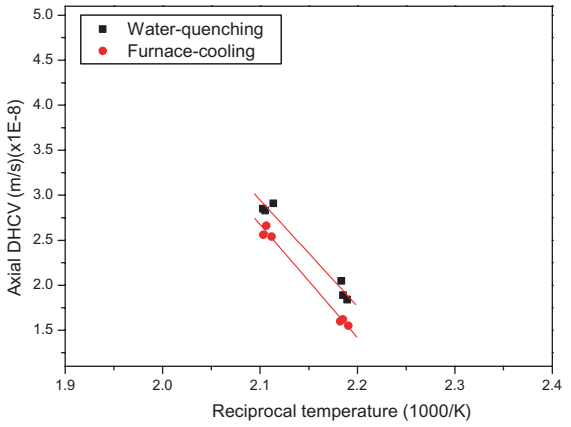

Fig. 13. Axial DHC velocity of Zr–2.5Nb tube subjected to water quenching and furnace cooling after homogenization treatment to dissolve 60 ppm H: the water-quenched compact tension specimens had slightly higher DHCV than the furnace-cooled.

However, this assumption is contradictory to the results shown in Figs. 12 and 13. Paradoxically, the results as shown in Figs. 12 and 13 demonstrate that the terminal solid solubility of hydrides for dissolution or precipitation are affected by the size of the hydrides as shown in Fig. 10 [8]. Some evidence for the effect of the hydride size on the dissolution has already been provided by Pan et al. who has experimentally confirmed that previous thermal history can significantly influence the value of the dissolution temperature [8].

Thus, during heating up to the peak temperature, 310 °C, the water-quenched and furnace-cooled specimens has the same concentration of hydrogen dissolved in the zirconium matrix (corresponding to the A′ and A point in Fig. 10, respectively). Upon reaching the test temperature or 250 °C by cooling, the tensile stress is applied to nucleate hydrides only at the crack tip with the supersaturated hydrogen concentration in solution, letting the crack tip reach the equilibrium hydrogen concentration corresponding to the C point (Fig. 10). Therefore, the hydrogen concentration dissolved at the crack tip region will be the same for both specimens independent of the hydride size as shown in Fig. 10. By contrast, the hydrogen concentration dissolved in the bulk region becomes higher for the water-quenched due to a larger amount of undercooling than that for the furnace-cooled specimens as shown in Fig. 10. In other words, it corresponds to the B′ point for the water-quenched specimens and to the B point for the furnace-cooled specimen (Fig. 10). Therefore, the concentration gradient between the bulk region and the crack tip becomes the distance B′C for the water-quenched specimen which is larger than the concentration gradient or BC for the furnace-cooled specimen (Fig. 10). However, the effect of the hydride size on the terminal solid solubility of hydrogen for dissolution and precipitation would be smaller as shown in Fig. 10 than TSSP–TSSD corresponding to a difference in the elastic accommodation energy arising from the hydride-matrix misfit between heat-up and cool-down [16–20]. This leads the water-quenched specimen to slightly higher DHC velocity than that of the furnace-cooled specimen.

4. Conclusion

The incubation time and velocity of DHC in CANDU Zr–2.5Nb tubes have been affected by the notch tip shape and the cooling rate. The incubation time of DHC had a gradual increase with the increased tip radius for the water-quenched and furnace cooled Zr–2.5Nb specimens and became larger for the furnace-cooled Zr–2.5Nb specimens with coarser hydrides than that for the water-quenched CB specimens especially at the notch tip radius larger than 0.125 mm. These results demonstrate that the incubation time is governed by the nucleation rate of reoriented hydrides at the notch tip that strongly depend on

the notch tip radius as well as the size of hydrides. A supplementary experiment verifies the faster nucleation of reoriented hydrides in the water-quenched Zr–2.5Nb specimens. Once the nucleation of hydrides turns the supersaturated hydrogen concentration to the equilibrium hydrogen concentration in solution, a constant concentration gradient is developed between the crack tip and the bulk region irrespective of the initial notch shape. This leads to a constant DHC velocity for the water-quenched or furnace-cooled Zr–2.5Nb as experimentally demonstrated in this study. Another thing is the effect of the size of hydrides on the terminal solid solubility of hydrides for dissolution and precipitation. During cooling-down from 310 °C to 250 °C at the same rate, the water-quenched specimens will have fine hydrides precipitated due to a memory effect, requiring a larger undercooling before the nucleation of hydrides and leading to the slightly higher TSSP curve compared to the furnace-cooled specimen. Thus, upon the nucleation of hydrides only at the crack tip under the applied tensile stress, reducing the supersaturated hydrogen concentration at the crack tip to the equilibrium hydrogen concentration for both water-quenched and furnace-cooled specimens, there develops a gradient of hydrogen concentration between the crack tip and the bulk region. However, the bulk region still maintains the supersaturated hydrogen concentration, the amount of which becomes larger for the water-quenched specimens due to the higher TSSP curve compared to the furnace-cooled specimen. Consequently, it leads the water-quenched specimen to have a slightly higher concentration gradient between the crack tip and the bulk region compared to the furnace-cooled specimen. This can explain why the water-quenched Zr–2.5Nb specimens had a slightly higher DHC velocity than the furnace-cooled specimens. As a conclusion, all the experimental results demonstrated in this study confirm that the Kim's DHC model is feasible.

Acknowldgments

This work has been carried out under the Nuclear R&D Program supported by Ministry of Science and Technology (MOST), Korea. One of the authors expresses sincere thanks to Drs Ian Ritchie and Kit Coleman for supplying information related to the DHC test procedures through an IAEA Coordinated Research Project 10376.

References

[1] R. Dutton, K. Nuttal, M.P. Puls, L.A. Simpson, Metall. Trans. 8A (1977) 1553.
[2] M.P. Puls, L.A. Simpson, R. Dutton, in: L.A. Simpson (Ed.), Fracture Problems and Solutions in the Energy Industry, Pergamon Press, Oxford, 1982, p. 13.
[3] C.E. Coleman, J.F.R. Ambler, Zirconium in the Nuclear IndustryASTM STP 633, American Society for Testing and Materials, 1977, p. 589.
[4] J.F.R. Ambler, Zirconium in the Nuclear Industry: Sixth International SymposiumASTM STP 824, American Society for Testing and Material, 1984, p. 635.
[5] K.F. Amouzouvi, L.J. Clegg, Metall. Trans. 18A (1987) 1687.
[6] Y.S. Kim, S.S. Park, S.S. Kim, Y.M. Cheong, K.S. Im, Proceedings of the Symposium on Zirconium-2002, p. 58.
[7] Y.S. Kim, in: TMS 2003 Annual Meeting & Exhibition Program and Guide: JOM 55, 2003, p. 383.
[8] Z.L. Pan, I.G. Ritchie, M.P. Puls, J. Nucl. Mater. 228 (1996) 227.
[9] M.P. Puls, Acta Metall. 29 (1981) 1961.
[10] D.J. Cameron, R.G. Duncan, J. Nucl. Mater. 68 (1977) 340.
[11] J.S. Bradbrook, G.W. Lorimer, N. Ridley, J. Nucl. Mater. 42 (1972) 142.
[12] Y.S. Kim et al., KAERI/TR-1329/99, Korea Atomic Energy Research Institute, Daejeon, 1999.
[13] A.D. Lepage, W.A. Ferris, G.A. Ledoux, AECL Report, FC-IAEA-03, TI.20.13-CAN-27363-03, 1998.
[14] S.J. Kim, Effect of Heat Treatment on Delayed Hydride Cracking Behavior of Zr–2.5%Nb Alloy, Master thesis, Korea University, 1999.
[15] S.S. Kim, Y.S. Kim, J. Nucl. Mater. 279 (2000) 286.
[16] M.P. Puls, Acta Metall. 32 (1984) 1259.
[17] C.E. Ells, J. Nucl. Mater. 28 (1968) 129.
[18] G.K. Shek, The effect of material properties, thermal and loading history on delayed hydride cracking in Zr–2.5Nb alloys, PhD thesis, The University of Manchester, 1998.
[19] R.L. Eadie, R.R. Smith, Can. Metall. Q. 27 (1988) 213.
[20] M.P. Puls, J. Nucl. Mater. 165 (1989) 128.